



# Examining the behavior of MHD micropolar fluid over curved stretching surface based on the modified Fourier law

A. Afsar Khan<sup>a,\*</sup>, R. Batool<sup>a</sup>, and N. Kousar<sup>b</sup>

a. *Department of Mathematics and Statistics, International Islamic University, Islamabad, 44000, Pakistan.*

b. *Department of Mathematics, FBAS, Air University, Islamabad, Pakistan.*

Received 24 July 2018; received in revised form 30 June 2019; accepted 12 October 2019

## KEYWORDS

Micropolar fluid;  
 MHD;  
 Cattaneo-Christov model;  
 Curved stretching surface;  
 Optimal homotopy analysis method.

**Abstract.** The present study describes Magneto hydrodynamic micropolar fluid over a curved stretching surface, based on Cattaneo-Christov theory of heat diffusion. In this paper, the new heat model with the relaxation time is employed in this paper, instead of classical theory of heat flux presented by Fourier. The curvilinear coordinates are used to model the governing equations. The nonlinear Partial Differential Equations (PDEs) are changed into Ordinary Differential Equations (ODEs) through a proper transformation process. The nonlinear ODEs are solved with the help of OHAM by using BVP4c. The variation of several parameters is indicated and examined graphically. We have observed that the pressure and velocity rises by increasing the radius of curvature. The thermal relaxation time and Prandtl number reduces the temperature profile.

© 2021 Sharif University of Technology. All rights reserved.

## 1. Introduction

Heat transfer is the movement of thermal energy from one object to another object with different temperature. It is an important area of research because of its different applications in various fields, including heat pumps, energy production and cooling systems of electronic devices, etc. The famous law of heat conduction was firstly suggested by Fourier [1]. The drawback of Fourier model is that it describes the parabolic energy equation, which gives the initial disturbance of the medium. To overcome this problem, a thermal relaxation time was introduced in Fourier law by Cattaneo [2]. It involves hyperbolic equation and gives finite speed of thermal signals. Different materials

have different relaxation time, that is why Christov [3] introduced the time derivative model called Oldroyd upper convected derivative. This heat flux model is called Cattaneo-Christov model. The uniqueness and structural stability of the Cattaneo-Christov has been examined by Ciarletta and Straughan [4]. Ostoja-Starzewski [5] described Maxwell Cattaneo equation by using material time derivative. The numerical study of Maxwell MHD flow of Cattaneo-Christov model has been examined by Shahid et al. [6]. Alamri et al. [7] discussed the possibility of employing Cattaneo-Christov model in a stretching cylinder.

The properties of non-Newtonian fluids are different from those of Newtonian fluid. Many materials show the non-Newtonian behavior, i.e., blood, apple sauce, toothpaste, paint etc. Non-Newtonian fluids are complex in nature and due to their rheological properties are involved in constitutive equation. These types of fluids are not described by single expression due to their various characteristics. Micropolar fluids are with micro structure. Eringen [8] developed the concept of

\*. *Corresponding author. Tel.: +92 300 5031398*  
*E-mail addresses: ambreen.afsar@iiu.edu.pk (A. Afsar Khan); nabeela@mail.au.edu.pk (N. Kousar)*

micropolar fluid and explained the behavior of certain fluids. Physically a micropolar fluid is one which contains suspensions of rigid particles. In previous years, the study of micropolar fluid has received a great deal of attention because of its numerous applications in industries like colloids and polymeric suspension, animal’s blood etc. The micro structural effect in the fluid was observed by Jeffery [9]. He showed that the presence of these particles cause the fluid velocity to be increased. Ericksen [10] introduced the field equations for micropolar fluid.

Flow caused by stretching surface is employed in extrusion process. Crane [11] found the solution of the stretching surface. The process of stretching occurs in the manufacturing processes of both polymer and metal sheets and paper production. The final production quality depends on the rate of heat transfer at the stretching surface. Following that, the numerical and analytical studies on stretching flow are reported in [12–23].

The purpose of this research is to explore the effect of magnetic field on micropolar fluid resulted from curved stretching surface. The Cattaneo-Christov heat model is used to formulate the problem. The resulting non-linear equations are solved by OHAM. The obtained series solutions are plotted graphically and discussed physically.

**2. Mathematical formulation**

The steady boundary layer flow of a micropolar fluid along a curved linearly stretching surface looped in a circle of radius  $R$  is considered. The origin  $O$  is fixed by applying two opposite and equal forces along the  $x$  direction and  $r$  is perpendicular to it. The magnetic field of strength  $B_0$  is imposed in the  $r$  direction. The temperature of surface is  $T_w$ , where  $T_w > T_\infty$  with  $T_\infty$  denoting ambient temperature of fluid. Under the above conditions, the governing equations are given as [21]:

$$\frac{\partial}{\partial r} \{ (r + R)v \} + R \frac{\partial u}{\partial x} = 0, \tag{1}$$

$$\frac{u^2}{r + R} = \frac{1}{\rho} \frac{\partial P}{\partial r}, \tag{2}$$

$$\begin{aligned} \nu \frac{\partial u}{\partial r} + \frac{Ru}{R+r} \frac{\partial u}{\partial x} + \frac{uv}{r+R} &= -\frac{1}{\rho} \frac{R}{(r+R)} \frac{\partial P}{\partial x} \\ &+ \left( \nu + \frac{K}{\rho} \right) \left( \frac{\partial^2 u}{\partial r^2} + \frac{1}{r+R} \frac{\partial u}{\partial r} - \frac{u}{(r+R)^2} \right) \\ &- \frac{K}{\rho} \frac{\partial N}{\partial r} - \frac{\sigma B_0^2}{\rho} u, \end{aligned} \tag{3}$$

$$\begin{aligned} v \frac{\partial N}{\partial r} + \frac{ru}{r+R} \frac{\partial N}{\partial x} &= \frac{\gamma^*}{\rho j} \left( \frac{\partial^2 N}{\partial r^2} + \frac{1}{r+R} \frac{\partial N}{\partial r} \right) \\ &- \frac{K}{\rho j} \left( 2N + \frac{\partial u}{\partial r} + \frac{u}{r+R} \right), \end{aligned} \tag{4}$$

$$\begin{aligned} v \frac{\partial T}{\partial r} + \frac{ru}{r+R} \frac{\partial T}{\partial x} + \alpha \left( v^2 \frac{\partial^2 T}{\partial r^2} + \frac{r^2 u^2}{(r+R)^2} \frac{\partial^2 T}{\partial x^2} \right. \\ \left. + \frac{2ruv}{r+R} \frac{\partial^2 T}{\partial x \partial r} - \frac{ruv}{(r+R)^2} \frac{\partial T}{\partial x} - v \frac{\partial T}{\partial r} \frac{\partial v}{\partial r} \right. \\ \left. + \frac{Ru}{r+R} \frac{\partial T}{\partial x} \frac{\partial v}{\partial r} \right) &= \frac{k}{\rho c_p} \left( \frac{\partial^2 T}{\partial r^2} + \frac{1}{r+R} \frac{\partial T}{\partial r} \right). \end{aligned} \tag{5}$$

According to the definition of spin gradient viscosity in the relevant professional literature:

$$\gamma^* = \left( \mu + \frac{K}{2} \right) j. \tag{6}$$

The boundary conditions for the problem is:

$$\begin{aligned} u = ax, \quad v = 0, \quad N = -m_0 \frac{\partial u}{\partial r}, \quad T = T_w, \\ \text{at } r = 0, \\ u \rightarrow 0, \quad \frac{\partial u}{\partial r} \rightarrow 0, \quad N \rightarrow 0, \quad T \rightarrow T_w, \\ \text{as } r \rightarrow \infty, \end{aligned} \tag{7}$$

where  $m_0$  ( $0 \leq m_0 \leq 1$ ) is a constant. We use the following similarity transformations into Eqs. (1) to (5):

$$\begin{aligned} u = axf'(\eta), \quad v = -\frac{R}{r+R} \sqrt{av} f'(\eta), \\ N = ax \sqrt{\frac{a}{v}} g, \quad \eta = \sqrt{\frac{a}{v}} r, \\ P = \rho a^2 x^2 P(\eta), \quad \theta(\eta) = \frac{T - T_\infty}{T_w - T_\infty}. \end{aligned} \tag{8}$$

By using the above transformations, Eq. (1) is satisfied identically. Eqs. (2)–(5) become:

$$\frac{\partial P}{\partial \eta} = \frac{(f')^2}{\eta + s'}, \tag{9}$$

$$\begin{aligned} \frac{2s}{\eta + s} P = (1 + W) \left[ f''' + \frac{f''}{\eta + s} - \frac{f'}{(\eta + s)^2} \right] \\ - \frac{s}{\eta + s} (f')^2 + \frac{s}{\eta + s} f f'' \\ + \frac{s}{(\eta + s)^2} f f' - W g' - M^2 f', \end{aligned} \tag{10}$$

$$\left(1 + \frac{W}{2}\right) \left[ g'' + \frac{g'}{\eta + s} \right] + \frac{s}{\eta + s} f g' - \frac{s}{\eta + s} f' g - W \left( 2g + f'' + \frac{f'}{\eta + s} \right) = 0, \quad (11)$$

$$\theta'' + \frac{\theta'}{\eta + s} + \text{Pr} \frac{s}{\eta + s} \theta' f - \text{Pr} \frac{s^2 \gamma}{(\eta + s)^2} [f^2 \theta'(\eta + s) - f f' \theta' + f^2 \theta''] = 0, \quad (12)$$

where  $W = \frac{K}{\nu}$ ,  $s = R\sqrt{\frac{\alpha}{\nu}}$ ,  $M = \sqrt{\frac{\sigma B_0^2}{\rho \alpha}}$ , and  $\text{Pr} = \frac{\mu c_p}{k}$ .

Pr is the Prandtl number,  $s$  is the radius of curvature,  $W$  is the material parameter, and  $M$  is the magnetic parameter.

Eliminating the pressure from Eqs. (9) and (10), we get:

$$f^{iv} + \frac{2f'''}{\eta + s} - \frac{f''}{(\eta + s)^2} + \frac{f'}{(\eta + s)^2} - \frac{s}{\eta + s} (f'' f' - f f''') - \frac{s}{(\eta + s)^2} (f'^2 - f'' f) - \frac{s}{(\eta + s)^2} f f' - M^2 \left( f''' + \frac{f'}{\eta + s} \right) = 0, \quad (13)$$

Pressure can be obtained from Eq. (10):

$$P = \frac{\eta + s}{2s} \left[ (1 + W) \left\{ f''' + \frac{f''}{\eta + s} - \frac{f'}{(\eta + s)^2} \right\} - \frac{s}{\eta + s} f'^2 + \frac{s}{\eta + s} f'' f - \frac{s}{(\eta + s)^2} f f' - W g' - M^2 f' \right]. \quad (14)$$

Boundary conditions are:

$$f(0) = 0, \quad f'(0) = 1, \quad g(0) = 0, \quad \theta(0) = 1, \\ f'(\infty) = 0, \quad f''(\infty) = 0, \quad g(\infty) = 0, \quad \theta(\infty) = 0. \quad (15)$$

The skin friction and couple stress coefficient are the physical quantities of interest, which are expressed as:

$$C_f = \frac{T_{rs}}{\rho u_w^2}, \quad C_m = \frac{M_w}{\mu j u_w}, \quad (16)$$

in which  $T_{rs}$  and  $M_w$  are the wall shear stress and wall couple stress respectively, which are given by:

$$M_w = \gamma^* \frac{\partial N}{\partial r} \quad \text{at } r = 0, \quad (17)$$

$$T_{rs} = (K + \mu) \left( \frac{\partial u}{\partial r} - \frac{u}{r + R} \right) + KN \quad \text{at } r = 0. \quad (18)$$

We use Eq. (8) into Eqs. (16) to (18). Eq. (16) becomes:

$$RC_f e_s^{\frac{1}{2}} = (1 + W) \left\{ f''(0) - \frac{f'(0)}{s} \right\}, \quad (19)$$

$$RC_m e_s = \left( 1 + \frac{W}{2} \right) g'(0). \quad (20)$$

### 3. Optimal homotopic solutions

We solve the above ODE's by using the optimal homotopy method. The initial guesses, linear operator and auxiliary functions for the velocity, micro rotation and heat equation are assumed as follows:

$$h_f = e^{-\eta} = h_g = h_\theta, \quad (21)$$

$$L_f = f^{iv} + f''', \quad L_g = g'' - g, \quad L_\theta = \theta'' - \theta, \quad (22)$$

$$f(0) = 1 - e^{-\eta}, \quad g(0) = \eta e^{-\eta}, \quad \theta(0) = e^{-\eta}. \quad (23)$$

The properties are:

$$L_f = C_1 + C_2 x + C_3 x^2 + C_4 e^{-\eta}, \quad (24)$$

$$L_g = C_5 e^\eta + C_6 e^{-\eta}, \quad (25)$$

$$L_\theta = C_7 e^\eta + C_8 e^{-\eta}. \quad (26)$$

The problem above in zero and  $n$ th order is:

$$(1 + t)L_f [\dot{f}(\eta, t) - f_0(\eta)] = t e_0^f N_f [\dot{f}(\eta, t)], \quad (27)$$

$$(1 + t)L_g [\bar{g}(\eta, t) - g_0(\eta)] = t e_0^g N_g [\bar{g}(\eta, t), \dot{f}(\eta, t)], \quad (28)$$

$$(1 + t)L_\theta [\Theta(\eta, t) - \theta_0(\eta)] = t e_0^\theta N_\theta [\bar{g}(\eta, t), \dot{f}(\eta, t)], \quad (29)$$

$$\dot{f}(\eta, t) = 0, \quad \frac{\partial \dot{f}(\eta, t)}{\partial \eta} = 1, \quad \Theta(\eta, t) = 1,$$

$$\bar{g}(\eta, t) = 0, \quad \text{at } \eta = 0,$$

$$\frac{\partial \dot{f}(\eta, t)}{\partial \eta} = 0, \quad \frac{\partial^2 \dot{f}(\eta, t)}{\partial \eta^2} = 0, \quad \Theta(\eta, t) = 0,$$

$$\bar{g}(\eta, t) = 0, \quad \text{at } \eta = \infty. \quad (30)$$

#### 3.1. Convergence analysis of solution

In order to achieve a monotonically convergent solution, we compute the square residual error for velocity, micro rotation and heat profile at different order of approximation as shown in Table 1.

**Table 1.** Averaged squared residual error using  $e_0^f = -0.2241$ ,  $e_0^g = -0.6912$ , and  $e_0^\theta = -0.7473$ .

Order of approximation	Velocity profile	Microrotation profile	Heat profile
2	0.0175963	0.944401	0.0089331
6	$1.71823 \times 10^{-8}$	0.000336992	0.000155282
8	$2.20359 \times 10^{-11}$	0.0000326767	0.0000292079
10	$3.44715 \times 10^{-14}$	$4.02022 \times 10^{-6}$	$6.19856 \times 10^{-6}$
16	$1.97832 \times 10^{22}$	$2.88388 \times 10^{-8}$	$9.19524 \times 10^{-8}$
18	$1.00026 \times 10^{-24}$	$7.44158 \times 10^{-9}$	$2.48415 \times 10^{-8}$
20	$3.12887 \times 10^{-27}$	$2.05994 \times 10^{-9}$	$6.92851 \times 10^{-9}$
22	$9.26106 \times 10^{-30}$	$5.9866 \times 10^{-10}$	$1.98329 \times 10^{-9}$
26	$1.53235 \times 10^{-34}$	$5.60164 \times 10^{-11}$	$1.72693 \times 10^{-10}$
28	$6.43954 \times 10^{-35}$	$1.78235 \times 10^{-11}$	$5.2201 \times 10^{-11}$
30	$2.60764 \times 10^{-36}$	$5.79454 \times 10^{-12}$	$1.59845 \times 10^{-11}$

**4. Results and discussion**

In this section, we compute the graphical impact of involved parameters, micro-rotation, velocity and temperature profile. Figure 1 shows the impact of  $M$  on velocity profile. We can see that velocity profile decreases when we raise the value of  $M$ . The magnetic force is a resistive quantity which works against the flow in response to decrease in velocity. In Figure 2, we analyzed the effect of material parameter on velocity. As the value of  $W$  increases the velocity also increases.

The influence of curvature on velocity profile is given in Figure 3; as shown in this figure the velocity increases with increase in the value of  $s$ . Figure 4 is plotted for impact of magnetic parameter on microrotation profile. As we can see, the micro-rotation profile decline by rising the value of  $M$ . Figure 5 illustrates the behavior of micro-rotation profile with curvature parameter. From this figure, it is clear that the micro-rotation profile increases as the value of  $s$  increases. Figure 6

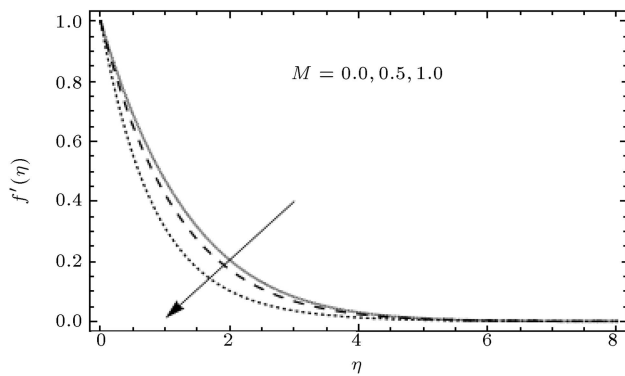


**Figure 1.** Effect of  $M$  when  $W = 1$  and  $s = 7$ .

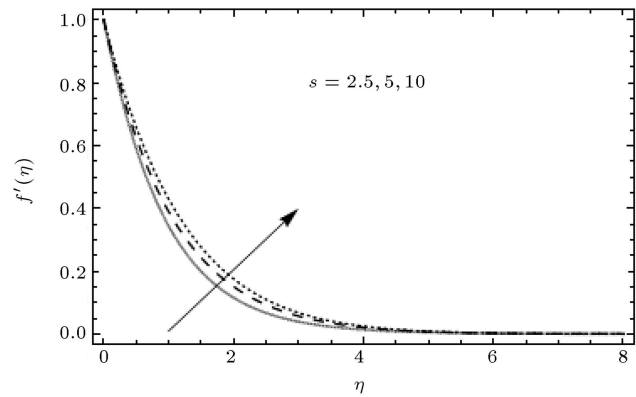


**Figure 3.** Effect of  $s$  when  $W$  and  $M = 0.8$ .

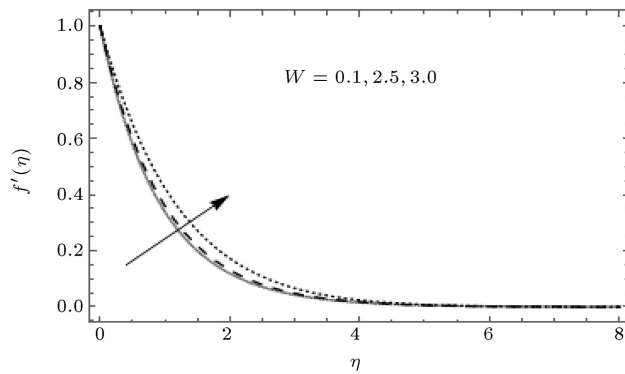


**Figure 2.** Effect of  $W$  when  $M = 0.5$  and  $s = 7$ .

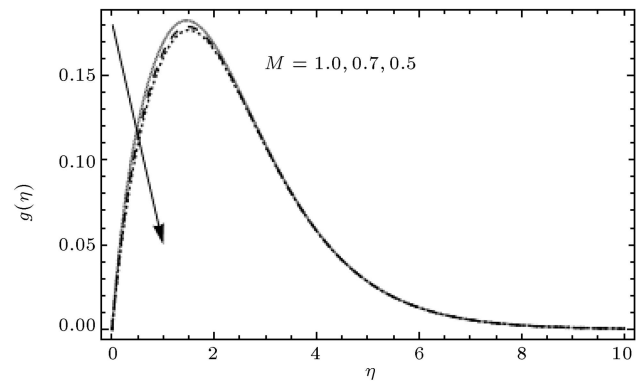


**Figure 4.** Effect of  $M$  profile when  $s = 7$  and  $W = 1$ .

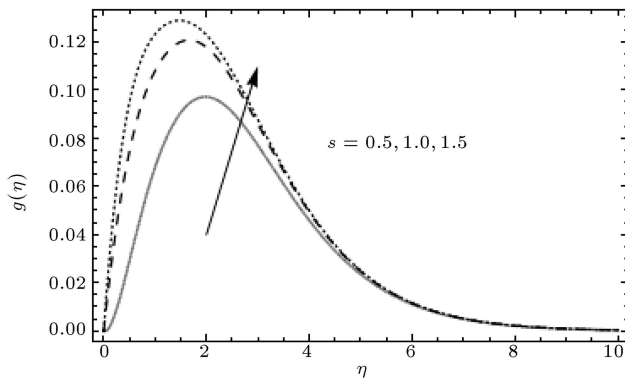


Figure 5. Effect of  $s$  when  $W = 3$  and  $M = 0.8$ .

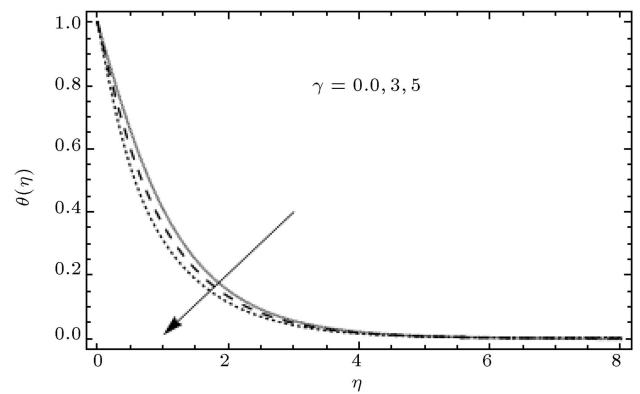


Figure 8. Effect of  $\gamma$  when  $s = 7$  and  $Pr = 1$ .

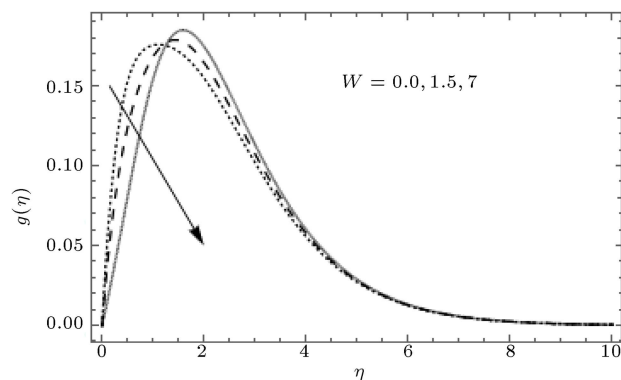


Figure 6. Effect of  $W$  when  $s = 7$  and  $M = 0.8$ .

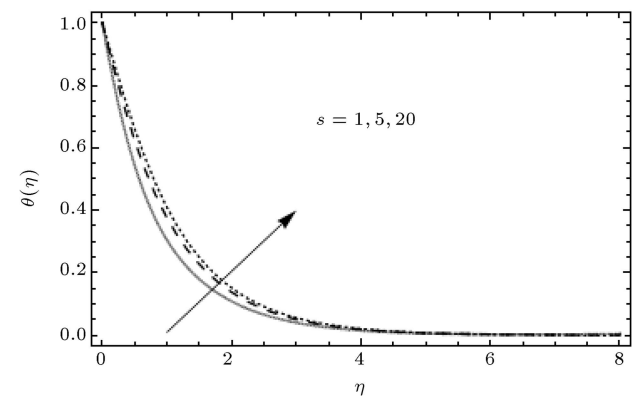


Figure 9. Effect of  $s$  when  $W = 2.5$  and  $\gamma = 0.6$ .

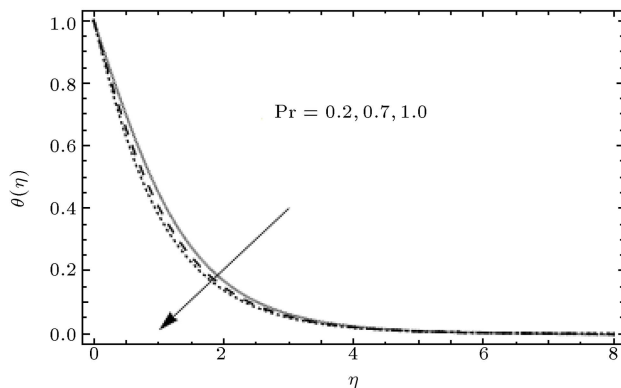


Figure 7. Effect of  $Pr$  when  $s = 7$  and  $\gamma = 0.5$ .

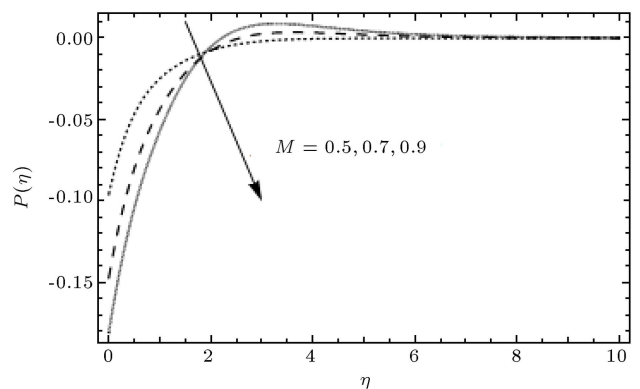


Figure 10. Effect of  $M$  when  $W = 7$  and  $s = 0.5$ .

explains the effect of  $W$  on microrotation profile. It is observed that micro-rotation profile increases with increase of  $W$ . From Figure 7, it can be noticed that the temperature profile shows decreasing behavior when we increase the  $Pr$ . Actually, the Prandtl number is the ratio between the thermal diffusivity and momentum diffusivity. We can observe from Figure 8 that the temperature profile decreases by increasing the value of  $\gamma$ . It means that more time is required to transfer energy from one particle to another particle by enhancing the thermal relaxation time. Figure 9 illustrates the impact of curvature parameter on temperature profile. We can see the temperature profile of fluid increases as

$s$  increases. Figure 10 represents the impact of  $M$  on the pressure of fluid. As  $M$  increases, the pressure of fluid decreases near the surface. In Figure 11, we can see that pressure increases by increasing the value of  $s$ . Figure 12 shows the effect of  $W$  on pressure, the similar effect is observed in Figure 10.

As shown in Table 2, to examine the validity and reliability of the results of the present study, they are compared with findings of Hayat and Qasim (2010) [17]. In this regard we assumed the flat stretching surface, by taking  $s \rightarrow \infty$ , i.e.,  $s = 1000$ . The results of the previous study was obtained using

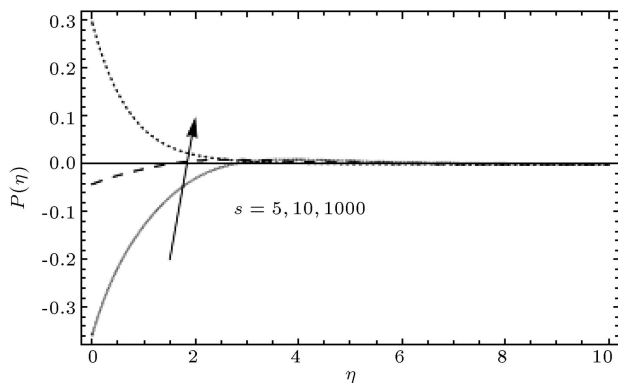


Figure 11. Effect of  $s$  when  $M = 1.5$  and  $W = 0.5$ .

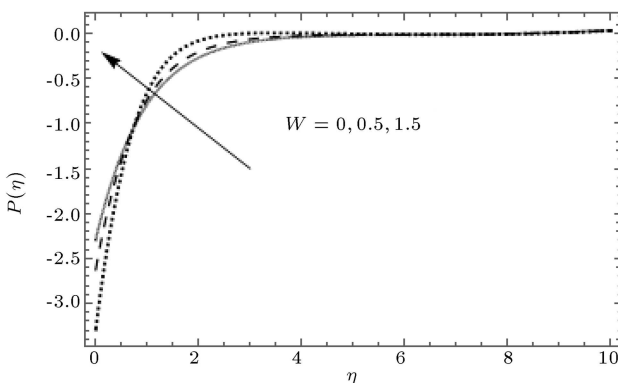


Figure 12. Effect of  $W$  when  $M = 1.5$  and  $s = 1.0$ .

HAM, while the numerical result of the present study was obtained using OHAM via BVP2 and in the present study the flat surface is considered. Table 3 presents the value of couple stress coefficient for the distinct values of  $M$  and  $W$  by fixing the  $s = 7$ . We have noticed that by enhancing the values of  $W$  and  $M$ , the  $RC_m e_s$  showed the increasing behavior. Regarding the value of heat transfer rate at surface, we observed that the heat transfer rate enhanced by enhancing the value of  $Pr$  and  $\gamma$  (Table 4).

Table 2. Comparison of numerical value of physical quantity  $Re_s^{1/2} C_f$  at different values of  $m$  and  $W$  with  $s = 1000$ .

$W$	$M$	Hayat and Qasim (2010)	Present study
0	0.5	1.1180	1.1182
1		1.5305	1.5307
2		1.8152	1.8153
4		2.2456	2.2454
1	0.0	1.3678	1.3679
	0.5	1.5305	1.5307
	1.0	1.9422	1.9424
	1.5	2.4873	2.4871

Table 3. Numerical result of couple stress coefficient for  $Re_s C_m$  at different values of  $W$  and  $m$  with  $s = 0.7$ .

$W$	$M$	$Re_s C_m$
0.3	0.1	0.239926
0.5		0.301092
1		0.45178
1	0.1	0.45178
	0.5	0.644904
	0.9	0.733538

Table 4. Value of heat transfer rate  $\theta'(0)$  at the surface  $s = 0.2$ .

$\gamma$	$Pr$	$-\theta'(0)$
0.0	1.0	1.90748
0.2		1.91475
0.4		1.92206
0.2	0.9	1.90167
	1.0	1.91475
	1.5	1.98096

### 5. Conclusions

In this study, we examined the MHD flow of a micropolar fluid over a curved stretching surface. The Cattaneo-Christov model has been implemented to see the thermal effect. The following observations may be extracted from the graphical results:

1. The pressure distribution increases by increasing  $M$ ,  $s$ , and  $W$  near the boundary of the curved surface and it tends to zero away from the boundary;
2. The microrotation and velocity of the fluid decrease by enhancing the value of  $M$ ;
3. The velocity and microrotation of the fluid increase by increasing the curvature parameter;
4. The temperature of the fluid is declined by enhancing the thermal relaxation time;
5. Future researchers need to consider the modified Fick's theory.

### Nomenclature

$P$	Pressure
$v$	Velocity in $r$ direction
$u$	Velocity in $x$ directions
$\sigma$	Electrical conductivity
$T$	Temperature
$N$	Micro-rotation parameter in the $rx$ -plane
$\gamma^*$	Spin gradient viscosity

$\rho$	Fluid density
$k$	Thermal conductivity
$K$	Vortex viscosity
$j$	Micro-inertial per unit mass
$\nu$	Kinematics viscosity of fluid
$\alpha$	Thermal relaxation time
$c_p$	Specific heat
$\mu$	Viscosity of fluid
$j = \frac{\nu}{ax}$	Reference length

## References

- Fourier, J.B.J., *Analytical Theory of Heat*, F. Didot (1822).
- Cattaneo, C. “Sulla conduzione del calore”, *Atti Sem. Mat. Fis. Univ. Modena*, **3**, pp. 83–101 (1948).
- Christov, C.I. “On frame indifferent formulation of the Maxwell-Cattaneo model of finite-speed heat conduction”, *Mechanics Research Communications*, **36**(4), pp. 481–486 (2009).
- Ciarletta, M. and Straughan, B. “Uniqueness and structural stability for the Cattaneo-Christov equations”, *Mechanics Research Communications*, **37**(5), pp. 445–447 (2010).
- Ostoja-Starzewski, M. “A derivation of the Maxwell-Cattaneo equation from the free energy and dissipation potentials”, *International Journal of Engineering Science*, **47**(7–8), pp. 807–810 (2009).
- Shahid, A., Bhatti, M.M., Bég, O.A., and Kadir, A. “Numerical study of radiative Maxwell viscoelastic magnetized flow from a stretching permeable sheet with the Cattaneo-Christov heat flux model”, *Neural Computing and Applications*, **30**, pp. 3467–3478 (2018). <https://doi.org/10.1007/s00521-017-2933-8>
- Alamri, S.Z., Khan A.A., Azeez, M., and Ellahi, R. “Effect of mass transfer on MHD second grade fluid towards stretching cylinder: A novel perspective of Cattaneo-Christov heat flux model”, *Physics Letter A*, **383**, pp. 276–281 (2019).
- Eringen, A.C. “Theory of micropolar fluids”, *Journal of Mathematics and Mechanics*, **16**(1), pp. 1–18 (1966).
- Jeffery, G.B. “The motion of ellipsoidal particles immersed in a viscous fluid”, *Proc. R. Soc. Lond. A*, **102**(715), pp. 161–179 (1922).
- Ericksen, J.L. “Anisotropic fluids”, *Arch. Ration. Mech. Anal.*, **4**(1), pp. 231–237 (1960).
- Crane, L.J. “Flow past a stretching plate”, *Zeitschrift für Angewandte Mathematik und Physik ZAMP*, **21**(4), pp. 645–647 (1970).
- Wang, C.Y. “The three-dimensional flow due to a stretching flat surface”, *AIP Phys. Fluid*, **27**, pp. 1915–1917 (1984).
- Waqas, M., Farooq, M., Khan, M.I., Alsaedi, A., Hayat, T., and Yasmeen, T. “Magnetohydrodynamic (MHD) mixed convection flow of micropolar liquid due to nonlinear stretched sheet with convective condition”, *International Journal of Heat and Mass Transfer*, **102**, pp. 766–772 (2016).
- Khan, W.A. and Pop, I. “Boundary-layer flow of a nano fluid past a stretching sheet”, *Int. J. Heat Mass Transf.*, **53**, pp. 2477–2483 (2010).
- Khan, A.A., Bukhari, S.R., and Marin, M. “Effect of chemical reaction on third grade MHD fluid flow under the influence of heat and mass transfer with variable reactive index”, *Heat Transfer Research*, **50**(11), pp. 1061–1080 (2019).
- Turkylmazoglu, M. “Dual and triple solution for MHD skip flow of non-Newtonian fluid over a shrinking surface”, *Comp & Fluid*, **70**, pp. 53–58 (2012).
- Hayat, T. and Qasim, M. “Effect of thermal radiation on unsteady magnetohydrodynamic flow of micropolar fluid with heat and mass transfer”, *Naturforsch.*, **65**(a), pp. 950–960 (2010).
- Turkylmazoglu, M. “Flow of a micropolar fluid due to a porous stretching sheet and heat transfer”, *International Journal of Non-Linear Mechanics*, **83**, pp. 59–64 (2016).
- Keimanesh, R. and Aghanajafi, C. “Analysis of radiation heat transfer of a micropolar fluid with variable properties over a stretching sheet in the presence of magnetic field”, *J. Heat Mass Transf.*, **1**, pp. 9–19 (2016).
- Saleh, S.H.M., Arifin, N.M., Nazar, R., and Pop, I. “Unsteady micropolar fluid over a permeable curved stretching shrinking surface”, *Mathematical Problems in Engineering*, **2017**, pp. 1–12 (2017). <https://doi.org/10.1155/2017/3085249>
- Turkylmazoglu, M. “Latitudinally deforming rotating sphere”, *Applied Mathematical Modelling*, **71**, pp. 1–11 (2019).
- Turkylmazoglu, M. “Convergence accelerating in the homotopy analysis method: A new approach”, *Advances in Applied Mathematics and Mechanics*, **10**(4), pp. 925–947 (2018).
- Naveed, M., Abbas, Z., and Sajid, M. “MHD flow of micropolar fluid due to a curved stretching sheet with thermal radiation”, *Journal of Applied Fluid Mechanics*, **9**(1), pp. 131–138 (2016).

## Biographies

**Ambreen Afsar Khan** received her PhD degree from the Department of Mathematics, Quaid-i-Azam University, Islamabad, Pakistan. She is an Assistant Professor at International Islamic University, Islamabad, Pakistan. Her numerous research articles in

the field of fluid mechanics and elasto-dynamics have been published in the reputable international journals. She has carried out two sponsored research projects through HEC under NRP.

**Rabia Batool** is working as a Research Scholar under the supervision of Dr. Afsar Khan in the Department

of Mathematics and Statistics, International Islamic University, Islamabad, Pakistan.

**Nabeela Kousar** is an Associate Professor at Air University, Islamabad, Pakistan. Her area of interest is fluid mechanics. She has many research articles, published in the reputable international journals.